

# The nonlinear mean-field model of nuclear matter II

— renormalized optical potential\*—

K. Miyazaki

## Abstract

The relativistic impulse optical model of nuclei is investigated using derivative coupling potential. We have found the suppression of the negative-energy propagation compared to the usual  $t\rho$  potential. However it can be taken into account by the renormalized potential in the Dirac equation. Thus the Dirac phenomenology is still valid.

Recent extensive developments of relativistic nuclear models [1] were strongly inspired by the success of the relativistic impulse optical model. The relativistic  $t\rho$  optical potential [2] was able to reproduce the polarization observables, the analyzing power and spin rotation function, of  $p+^{40}\text{Ca}$  elastic scattering at 500 MeV, while the corresponding nonrelativistic potential failed. This success was attributed to the negative-energy propagation [3] in the Dirac equation. However it was claimed [4] that the negative-energy contribution should be suppressed due to the structure of a nucleon. This is a controversial problem [5] until now.

Recently, the author investigated [6] the effect of meson cloud surrounding a nucleon in nuclear matter. It produces the polarizabilities [7] of a nucleon in the medium. The polarizabilities are also derived by the derivative coupling model [8-10]. Because the meson cloud constitutes the structure of a nucleon, an application of the derivative coupling potential to the optical model is worthwhile to investigate the effect of nucleon structure on the negative-energy propagation. In order to introduce the derivative coupling potential into the relativistic impulse optical model, we utilize a fundamental ambiguity [11] in the  $t\rho$  potentials. Usually, the Fermi covariant representation is used for a relativistic NN  $t$ -matrix in the model. The five invariant amplitudes are determined to reproduce free NN scattering data. We can therefore multiply the  $t$ -matrix by any operator  $\Lambda(p)$ , which satisfies  $\Lambda(p)u(p) = u(p)$  for the free positive-energy Dirac spinor  $u(p)$ . It cannot be excluded to replace the  $t\rho$  optical potential  $U$  by  $U\Lambda(p)$ .

If the scalar part  $S$  of  $U$  is considered and  $\Lambda(p)$  is given by

$$\Lambda(p) = \frac{\not{p} + M}{2M}, \quad (1)$$

---

\*This paper is the revised version of CDS ext-2002-068. Some texts and mistypes have been corrected.

we have

$$S\Lambda(p) = \frac{1}{2}S\frac{\not{p}}{M} + \frac{1}{2}S, \quad (2)$$

where  $M$  is the mass of a nucleon and  $p$  is its four momentum. This is just the hybrid derivative scalar coupling in Ref. [8]. More general derivative coupling in Ref. [9] can be derived by introducing the operator

$$\Lambda_\lambda(p) = \frac{\not{p} + M}{2M} + \lambda \frac{-\not{p} + M}{2M} \quad (3)$$

in place of Eq. (1). Then we have

$$S\Lambda_\lambda(p) = \frac{1-\lambda}{2}S\frac{\not{p}}{M} + \frac{1+\lambda}{2}S, \quad (4)$$

where  $\lambda$  is an appropriate parameter. Equation (4) reduces to Eq. (2) at  $\lambda = 0$  and to  $S$  at  $\lambda = 1$ . If  $\lambda = -1$ , it is equivalent to pure derivative scalar coupling [10] by Zimanyi and Moszkowsky.

Taking into account the vector potential, we have the following equation for N-A elastic scattering<sup>1</sup>

$$[\not{p} - M - (S_{(0)} + \gamma^0 V_{(0)})\Lambda_\lambda(p)]\psi = 0, \quad (5)$$

where  $S_{(0)}$  and  $V_{(0)}$  are the scalar and vector parts of the original  $t\rho$  potential. Equation (5) can be transformed to the equivalent Dirac equation,

$$[\not{p} - M - (S + \gamma^0 V)]\psi = 0 \quad (6)$$

with the renormalized scalar  $S$  and vector  $V$  potential given by

$$\frac{S}{M} = \frac{s_{(0)} + \lambda_- (v_{(0)}^2 - s_{(0)}^2)}{(1 - \lambda_- s_{(0)})^2 - (\lambda_- v_{(0)})^2}, \quad (7)$$

$$\frac{V}{M} = \frac{v_{(0)}}{(1 - \lambda_- s_{(0)})^2 - (\lambda_- v_{(0)})^2}, \quad (8)$$

where  $s_{(0)} = S_{(0)}/M$ ,  $v_{(0)} = V_{(0)}/M$  and  $\lambda_- = (1 - \lambda)/2$  [17]. To the second order of  $s_{(0)}$  and  $v_{(0)}$ , Eqs. (7) and (8) become

$$S/M \approx s_{(0)} + \lambda_- (s_{(0)}^2 + v_{(0)}^2), \quad (9)$$

---

<sup>1</sup>We can consider another potential  $\Lambda_\lambda(p)U$  in Eq. (5). However this describes the same scattering as  $U\Lambda_\lambda(p)$  by introducing the renormalized wave function that is asymptotically equivalent to  $\psi$  in Eq. (5). Similarly, we can consider a potential  $(1/2)(\Lambda_\lambda(p)U + U\Lambda_\lambda(p))$ . Because this is a sum of the above two potentials, it also describes the same scattering as them.

$$V/M \approx v_{(0)} + 2\lambda_- s_{(0)} v_{(0)}. \quad (10)$$

These accord with Eqs. (84) and (85) in Ref. [6]. The second and third term of r.h.s. in Eq. (9) and the second term of r.h.s. in Eq. (10) are just *the scalar polarizability*, *vector polarizability* and *the mixed scalar-vector polarizability* in Ref. [7] respectively. They are the first-order corrections to the  $t\rho$  potentials by the meson cloud surrounding a nucleon in the medium. In the investigation of nuclear matter saturation properties in Ref. [6], it was found that  $2\lambda_- = 0.35$ . This value is related to the isoscalar anomalous magnetic moment of a nucleon.

Equations (9) and (10) indicate that the polarizabilities reduce the strengths of  $t\rho$  potentials. In Figs. 1 and 2 we show the strengths of the real parts of  $p+^{40}\text{Ca}$  optical potentials as functions of proton incident-energy  $T_{LAB} \leq 1$  GeV. The dotted-dashed curves are the original  $t\rho$  potentials  $S_{(0)}$  and  $V_{(0)}$  calculated following Ref. [12]. The solid curves are the renormalized potentials (7) and (8) using  $\lambda_- = 0.18$ . They are compared with the phenomenological potentials. The dashed curves are the results by Ref. [13] and the triangles are from Ref. [14]. (We have used the parameter set 1 in Ref. [13] and 2, 3, 4, 5, 7, 9 and 13 in Ref. [14].) The triangles at  $T_{LAB} = 300$  and 400 MeV lie almost on the dashed curves. The other triangles can be fitted by the dotted curves that are 3d polynomials of  $(1/T_{LAB})$ . We see that the phenomenological potentials are determined uniquely only at  $T_{LAB} = 200$  and 800 MeV. However the potential strengths at 800 MeV have to be enhanced from the  $t\rho$  calculations and cannot be explained by the polarizabilities. The mechanism of such an enhancement is out of the present study. On the other hand, the renormalized potentials reproduce the triangles well below 200 MeV. Especially at 200 MeV, it agrees with both the phenomenological potentials. This indicates that the reduction of  $t\rho$  potentials by the polarizabilities is physically reasonable and supports the investigation of Ref. [6].

An essential ingredient of relativistic optical models is the so-called  $N\bar{N}$  pair effect [11] or the Z-graph contribution. It arises from negative-energy propagation and is the second-order contribution of the potentials. Therefore the polarizabilities in Eqs. (9) and (10) affect the negative-energy propagation. In order to investigate the difference between the original and renormalized  $t\rho$  potentials in the view of negative-energy propagation, we remember the work [15] by Cooper and Jennings. They studied its effect in the Dirac equation using the following propagator,

$$G^{(\eta)}(\mathbf{r}) \equiv G^{(+)}(\mathbf{r}) + \eta G^{(-)}(\mathbf{r}), \quad (11)$$

where  $G^{(\pm)}(\mathbf{r})$  is the positive and negative-energy part of the Feynman propagator, and  $0 \leq \eta \leq 1$  is a parameter. At  $\eta = 1$ , the full Feynman propagator is recovered, while the negative-energy propagation is suppressed for  $\eta < 1$ . Using the propagator (11) in the Lippmann-Schwinger equation for the scattering of a nucleon, Ref. [15] obtained Dirac

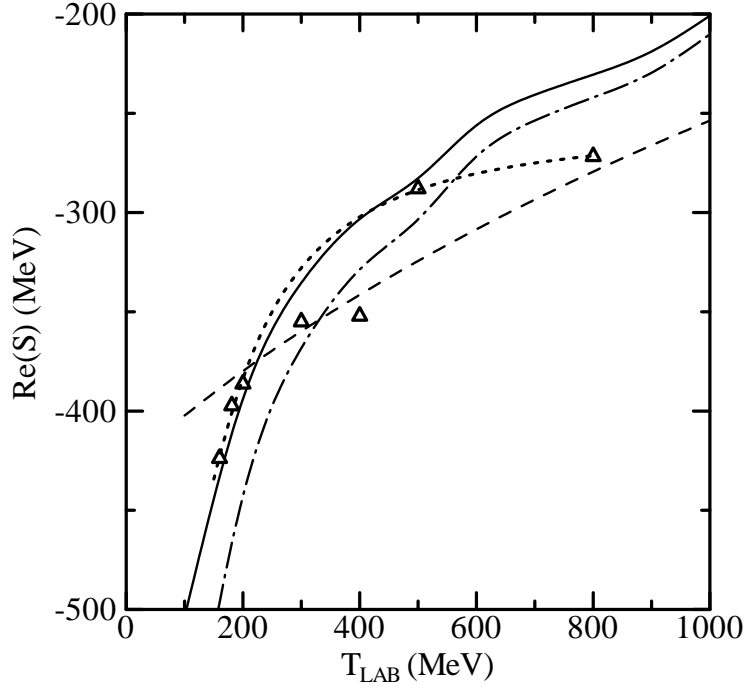


Figure 1: Strength of the real part of the scalar potential for  $p+^{40}\text{Ca}$  elastic scattering as a function of the proton incident-energy  $T_{LAB}$ . The dotted-dashed and solid curves are the original and renormalized  $t\rho$  potentials with  $\lambda_- = 0.18$  respectively. The dashed curve and the triangles are the phenomenological potentials of Ref. [13] and [14] respectively. The dotted curve is a fitting of the triangles except  $T_{LAB} = 300$  and  $400$  MeV by a 3d polynomial of  $(1/T_{LAB})$ .

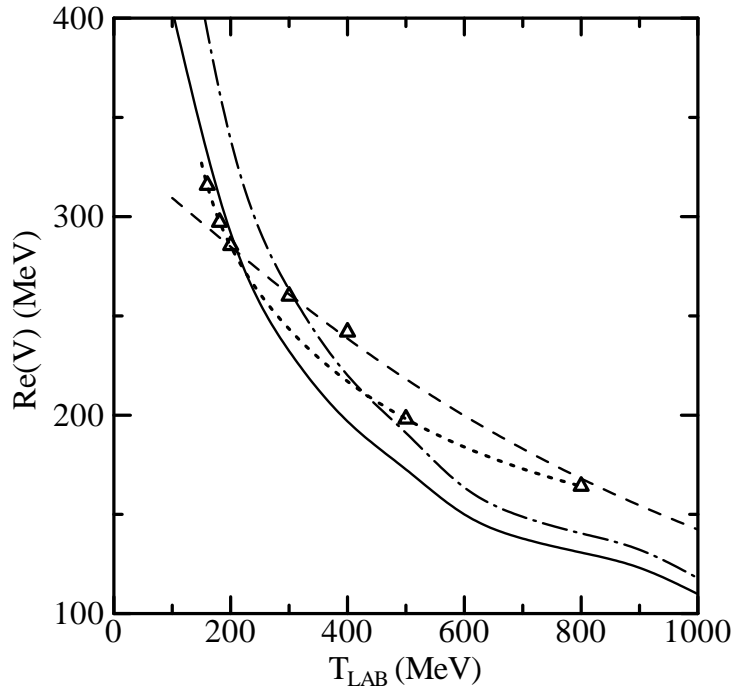


Figure 2: The same as Fig. 1 but for the vector potential.

equivalent equation with the effective scalar and vector potentials given by

$$\frac{S}{E} = \frac{\tilde{s}_{(0)}}{\left(1 + \eta_- \tilde{v}_{(0)}\right)^2 - \left(\eta_- \tilde{s}_{(0)}\right)^2}, \quad (12)$$

$$\frac{V}{E} = \frac{\tilde{v}_{(0)} + \eta_- \left(\tilde{v}_{(0)}^2 - \tilde{s}_{(0)}^2\right)}{\left(1 + \eta_- \tilde{v}_{(0)}\right)^2 - \left(\eta_- \tilde{s}_{(0)}\right)^2}, \quad (13)$$

where  $E$  is the center-of-mass energy of a nucleon in N+A system,  $\tilde{s}_{(0)} = S_{(0)}/E$ ,  $\tilde{v}_{(0)} = V_{(0)}/E$  and  $\eta_- = (1-\eta)/2$ . Expanding these expressions as in Eqs. (9) and (10), it is seen that the second-order contributions reduce the strengths of  $S$  and  $V$  for  $\eta < 1$  and have the same effect as the polarizabilities.

We want to determine the parameter  $\eta$  that is a measure of the suppression of negative-energy propagation. For this purpose, it is convenient to equate the ratio  $V/S$  obtained from Eqs. (7) and (8) with that from Eqs. (12) and (13). Then we have the relation between the parameter  $\eta$  and the polarizability  $\lambda_-$  as

$$\eta_- = - \frac{E V_{(0)}}{M S_{(0)} - \lambda_- \left(S_{(0)}^2 - V_{(0)}^2\right)} \lambda_-. \quad (14)$$

If there are no polarizabilities ( $\lambda_- = 0$ ),  $\eta$  returns to 1. Since  $\eta$  is a real quantity, Eq. (14) has a meaning only if the imaginary part of the r.h.s. can be negligible as compared with its real part. In Fig. 3 the solid curve shows  $\Re(\eta)$  as a function of  $T_{LAB}$  and the dashed curve is  $\Im(\eta)$  multiplied by 10. (In the calculation  $E$  is replaced by laboratory energy because the value of  $\lambda_-$  is determined for nuclear matter.) Here we assume that Eq. (14) is valid if the imaginary part is smaller than 1/10 of the real part. Thus the solid curve is meaningful at  $T_{LAB}$  below 500 MeV where it is almost constant. In the light of the results of Figs. 1 and 2, it is most reasonable to determine a value of  $\eta$  at  $T_{LAB} = 200$  MeV. We obtain  $\eta = 0.668 \simeq 2/3$ . This value is not precise because Eqs. (12) and (13) are derived by an assumption that the negative-energy propagation is approximately zero-ranged function. Nevertheless, it really means the suppression of negative-energy propagation by the polarizabilities in comparison with the original  $t\rho$  potential. The derivative coupling potential supplements the  $t\rho$  potential with the effect of nucleon structure by the meson cloud, which is realized in the polarizabilities of Eqs. (9) and (10). We can therefore conclude that the structure of a nucleon has the effect to suppress the negative-energy propagation in the Dirac phenomenology. This is consistent to the result of Ref. [16] that the longitudinal response of quasi-elastic electron-nucleus scattering is well described by relativistic mean-field model supplemented with the suppression of Z-graph contribution due to nucleon structure. It is however noted that the suppression can be incorporated into the renormalized potentials of Eqs. (7) and

(8), and so the Dirac phenomenology is seemingly valid against the criticism to it. The anomalous magnetic moment of a nucleon is the similar case. It is the result of nucleon structure but is taken in the Dirac representation of a nucleon through the Pauli term. In fact the polarizability  $\lambda_-$  is related to the isoscalar magnetic moment [6].

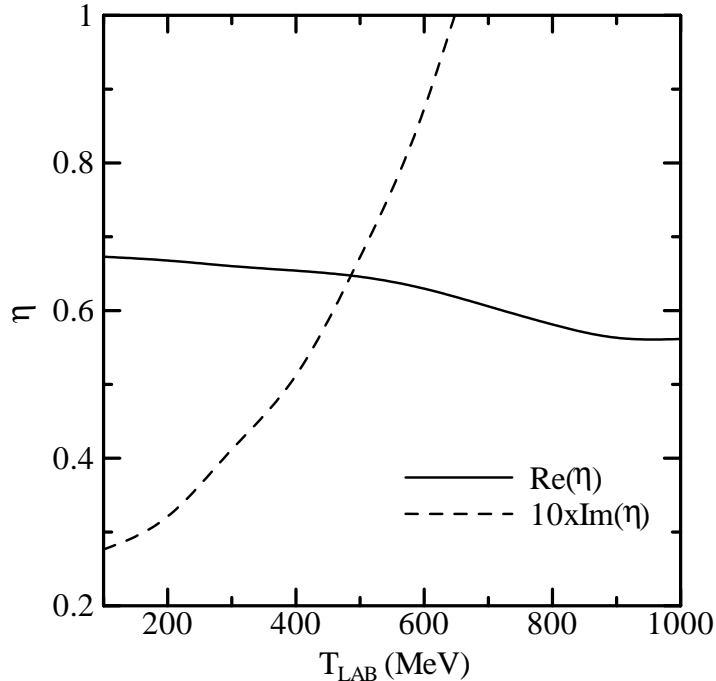


Figure 3: The r.h.s. of Eq. (14) as a function of the proton incident-energy  $T_{LAB}$ . The solid curve is its real part and the dashed curve is the imaginary part multiplied by 10.

We have applied the derivative coupling potential, which incorporates the effect of nucleon structure by the meson cloud, to the relativistic impulse optical model. It produces the renormalized optical potential that adds the polarizabilities of a nucleon to the  $t\rho$  potential. They improve the  $t\rho$  model for  $p+^{40}\text{Ca}$  elastic scattering around the incident energy of 200 MeV. Analyzing their effect in comparison to the work by Cooper and Jennings, it is found that the negative-energy propagation in the Dirac phenomenology is suppressed due to the structure of a nucleon.

## References

- [1] R.J. Furnstahl and B.D. Serot, arXiv:nucl-th/0005072,
- [2] J.A. McNeil, J.R. Shepard and S.J. Wallace, Phys. Rev. Lett. **50**, 1439 (1983); J.R. Shepard, J.A. McNeil and S.J. Wallace, Phys. Rev. Lett. **50**, 1443 (1983); B.C. Clark, S. Hama, R.L. Mercer, L. Ray and B.D. Serot, Phys. Rev. Lett. **50**, 1644 (1983).
- [3] M.V. Hynes, A. Picklesimer, P.C. Tandy and R.M. Thaler, Phys. Rev. **C31**, 1438 (1985).
- [4] M. Thies, Phys. Lett. **162B**, 255 (1985); T. Jaroszewicz and S.J. Brodsky, Phys. Rev. **C43**, 1946 (1991).
- [5] S.J. Wallace, Franz Gross and J.A. Tjon, Phys. Rev. Lett. **74**, 228 (1995); D.R. Phillips, M.C. Birse and S.J. Wallace, arXiv:nucl-th/9610007.
- [6] K. Miyazaki, CERN Document Server (CDS) ext-2002-056 revised by Mathematical Physics Preprint Archive (mp\_arc) 05-141.
- [7] M.C. Birse, Phys.Rev. **C51**, R1083 (1995).
- [8] N.K. Glendenning, F. Weber and S.A. Moszkowski, Phys. Rev. **C14**, 844 (1992).
- [9] S. Sarkar and B. Malakar, Phys. Rev. **C50**, 757 (1994).
- [10] J. Zimany and S.A. Moszkowski, Phys. Rev. **C42**, 1416 (1990).
- [11] J.A. Tjon and S.J. Wallace, Phys. Rev. **C32**, 267 (1985).
- [12] S.J. Wallace and J.L. Friar, Phys. Rev. **C29**, 956 (1984).
- [13] S. Hama, B.C. Clark, E.D. Cooper, H.S. Sherif, R.L. Mercer, Phys. Rev. **C41**, 2737 (1990).
- [14] A.M. Kobos, E.D. Cooper, J.I. Johansson and H.S. Sherif, Nucl. Phys. **A445**, 605 (1985).
- [15] E.D. Cooper and B.K. Jennings, Nucl. Phys. **A458**, 717 (1986).
- [16] K. Miyazaki, CERN Document Server (CDS) ext-2002-049 revised by Mathematical Physics Preprint Archive (mp\_arc) 05-150.